Supporting information

Hierarchically Porous Co-N-C Electrocatalysts with Enhanced Mass Transport and Cobalt Utilization Efficiency for Oxygen Reduction Reaction in High-Performance PEMFCs

Jinhyuk Baek[a], *Hyeonwook Son*[a], *Eungjun Lee*[b], *Sung Jong Yoo*[b], *Moonsu Kim*[a,c,*], *and Gibaek Lee*[a,*]

a: Advanced Energy Materials Design Lab., School of Chemical Engineering, Yeungnam University, 38541 Gyeongsan, Republic of Korea

b: Center for Hydrogen and Fuel Cells, Korea Institute of Science and Technology (KIST), 02792 Seoul, Republic of Korea

c: School of Advanced Materials and Electrical Engineering, Gyeongkuk National University, 36729 Andong, Republic of Korea

[*]Corresponding authors

To whom correspondence should be addressed.

E-mail: moonsukim@gknu.ac.kr (Prof. Moonsu Kim), gibaek@ynu.ac.kr (Prof. Gibaek Lee)

Tel.: +82+54-820-5754 (Prof. M. Kim); +82-53-810-2527 (Prof. G. Lee)

Fax: +82-53-810-4631 (Prof. G. Lee)

1. Supporting information

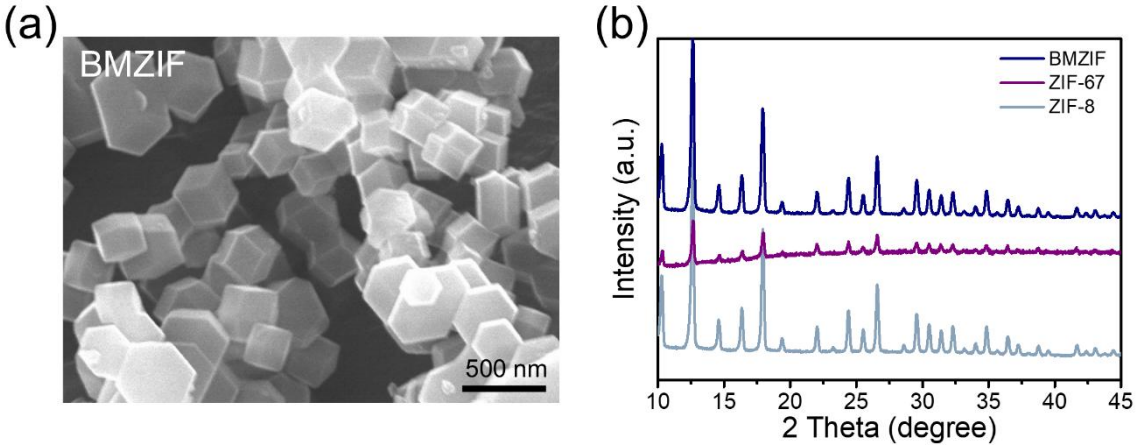

Figure S1. (a) SEM image of BMZIFs. (b) XRD patterns of BMZIF, ZIF-67, and ZIF-8.

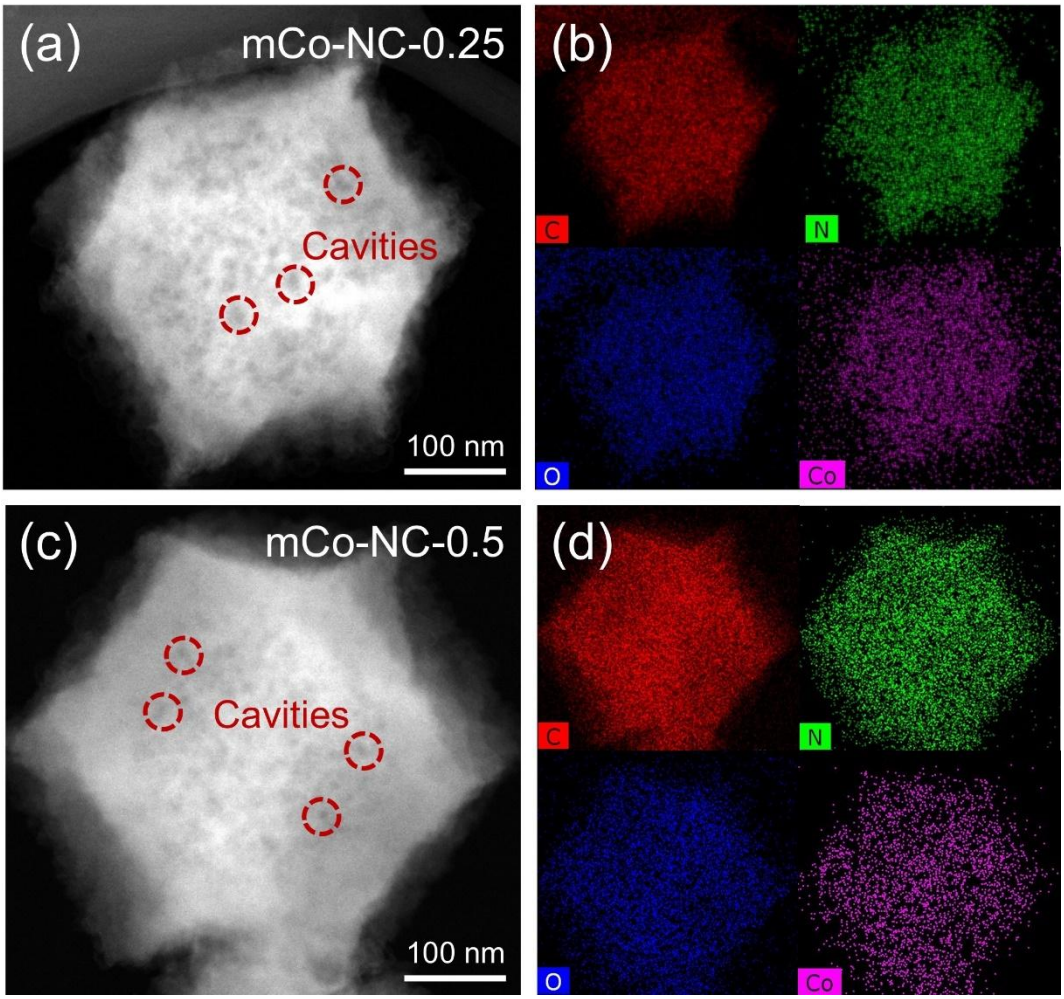

Figure S2. HAADF STEM images and corresponding EDS elemental mapping of (a, c) mCo-NC-0.25 and (b, d) mCo-NC-0.5.

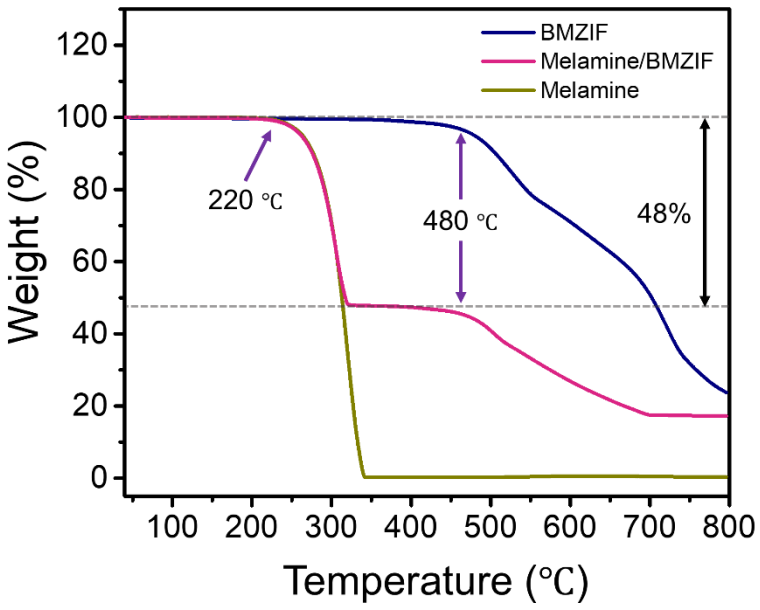

Figure S3. TGA curves of BMZIF, melamine, and melamine/BMZIF.

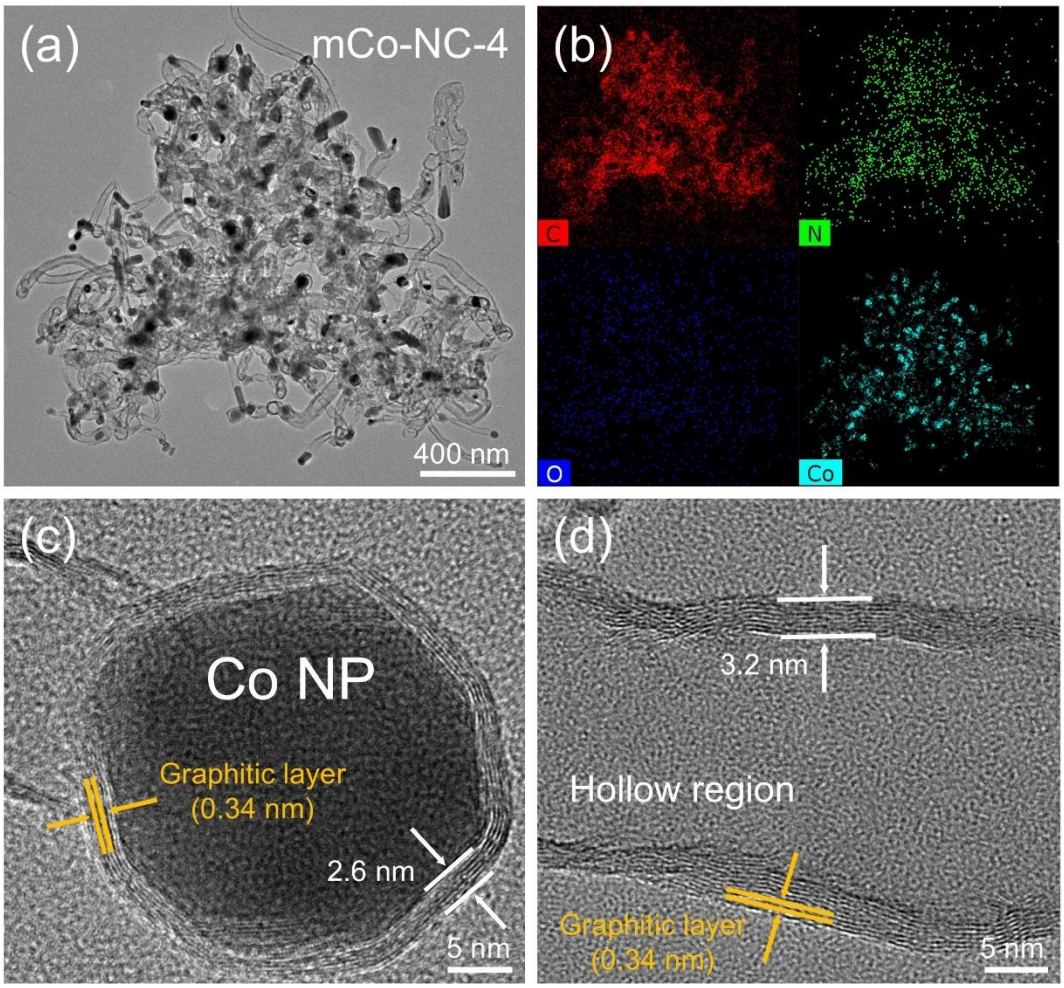

Figure S4. (a) TEM image, (b) EDS elemental mapping, and (c, d) HR-TEM images of mCo-NC-4.

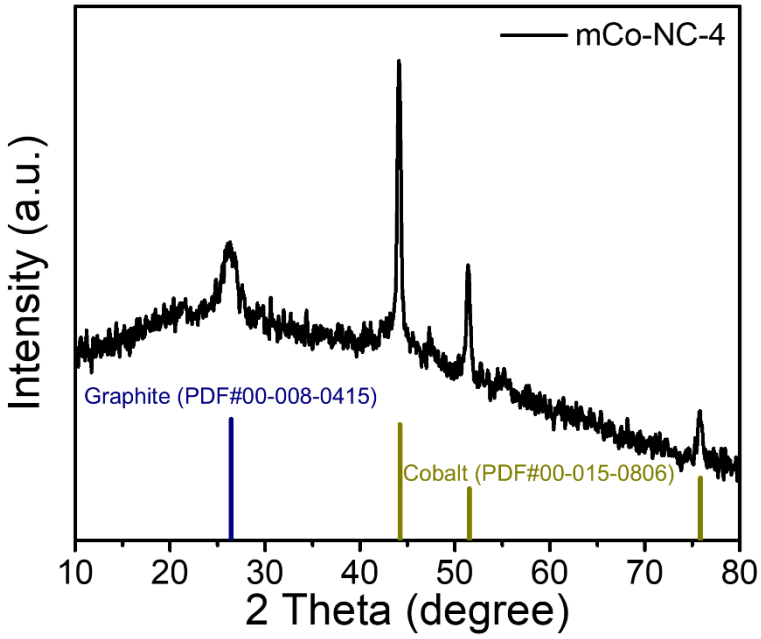

Figure S5. XRD pattern of mCo-NC-4.

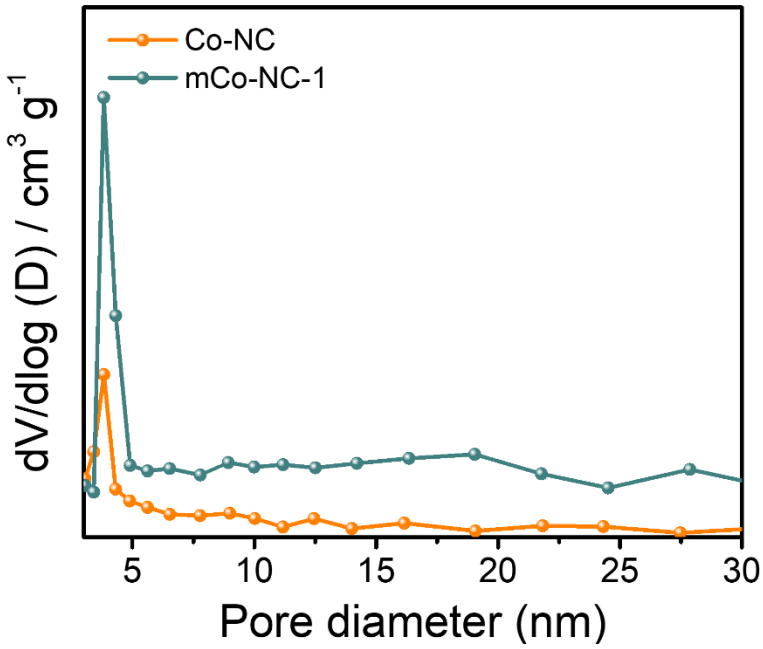

Figure S6. Pore size distribution of Co-NC and mCo-NC-1.

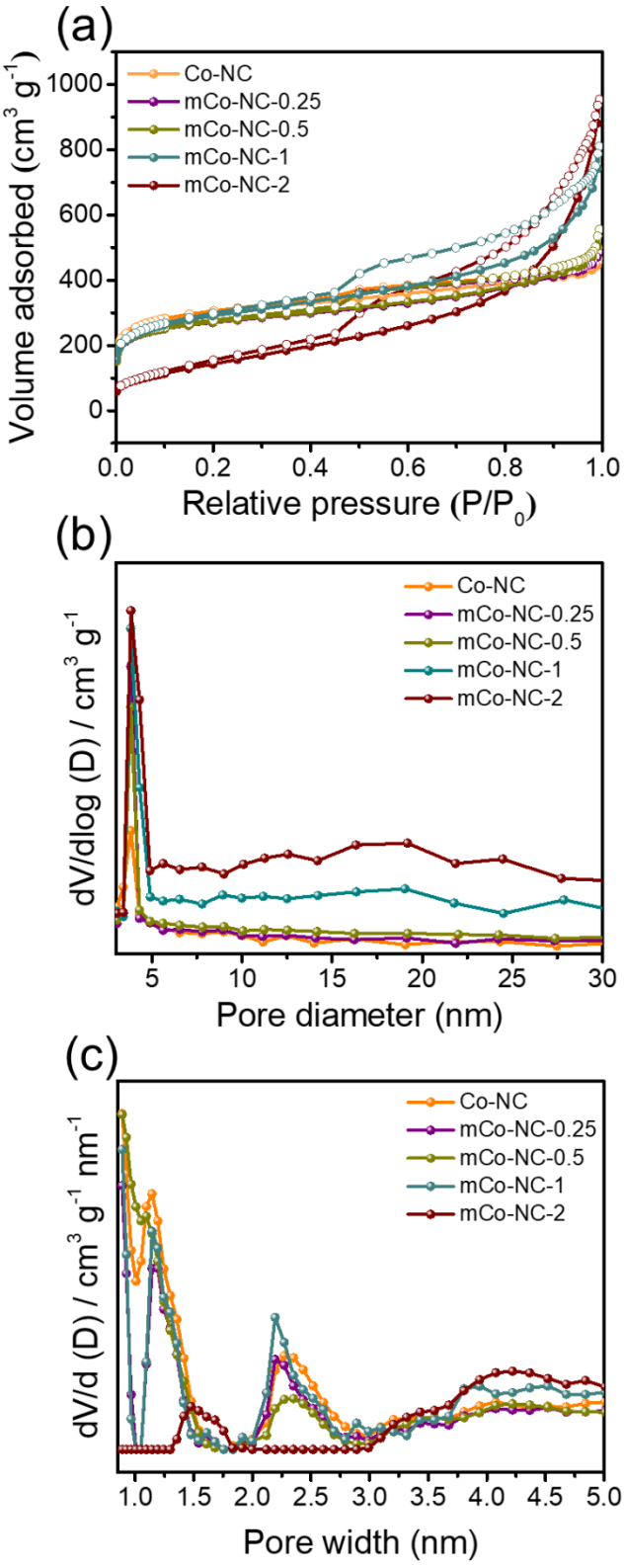

Figure S7. (a) N_2 adsorption-desorption isotherms and (b, c) corresponding pore size distribution of all catalysts.

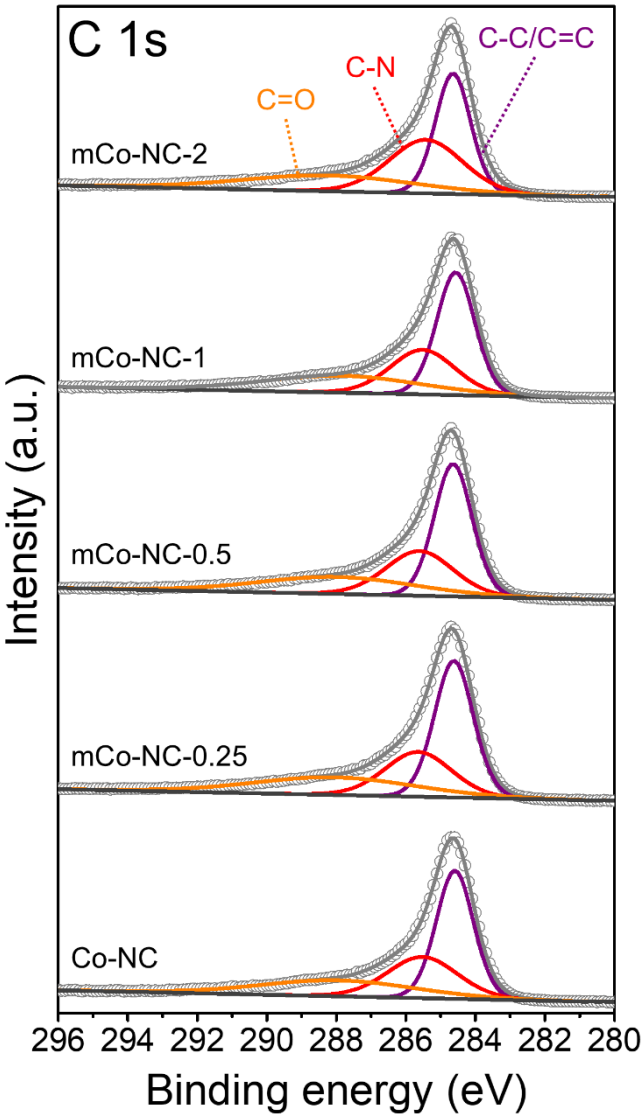

Figure S8. High-resolution C 1s XPS spectra of all catalysts.

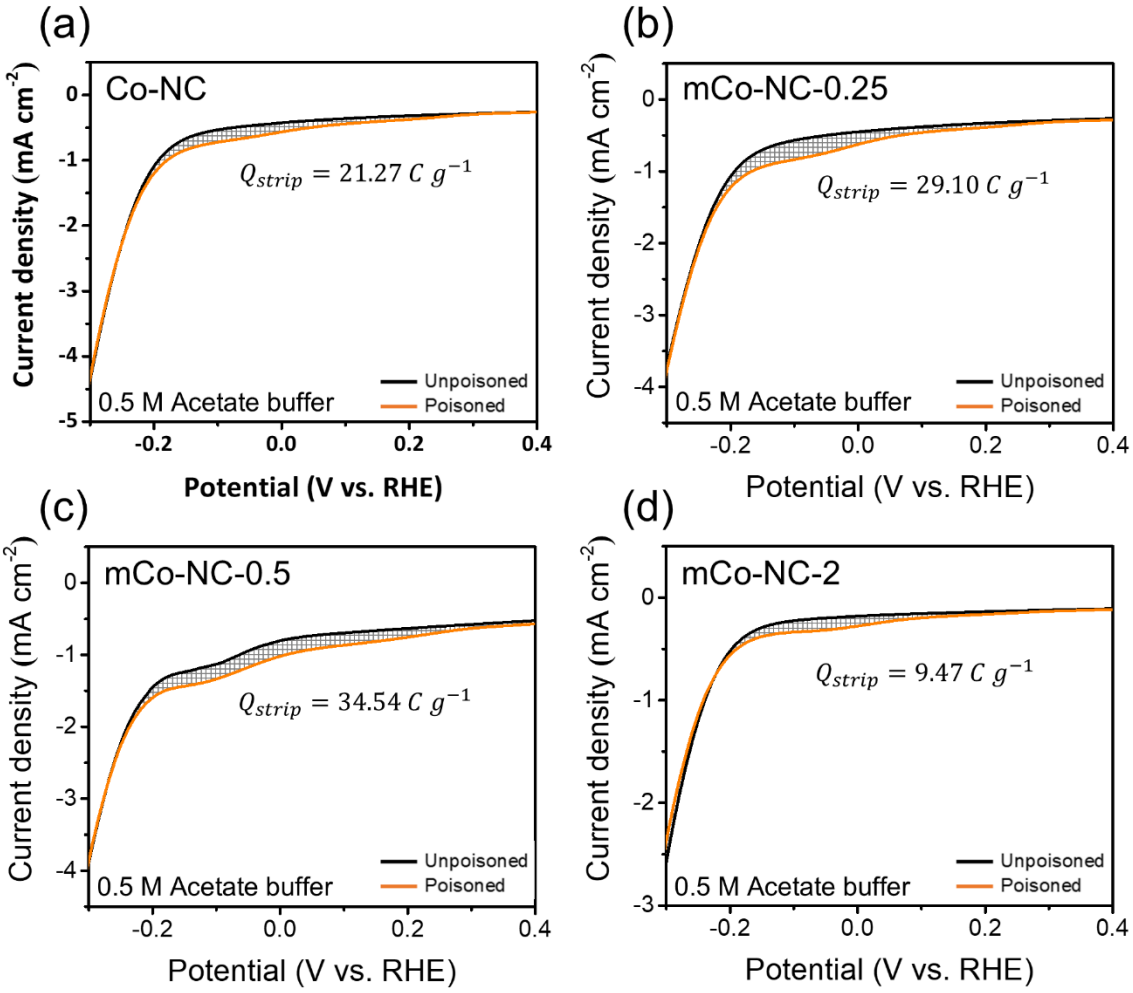

Figure S9. CV curves of nitrite adsorption/desorption for active site density measurement. (a) Co-NC, (b) mCo-NC-0.25, (c) mCo-NC-0.5, and (d) mCo-NC-2.

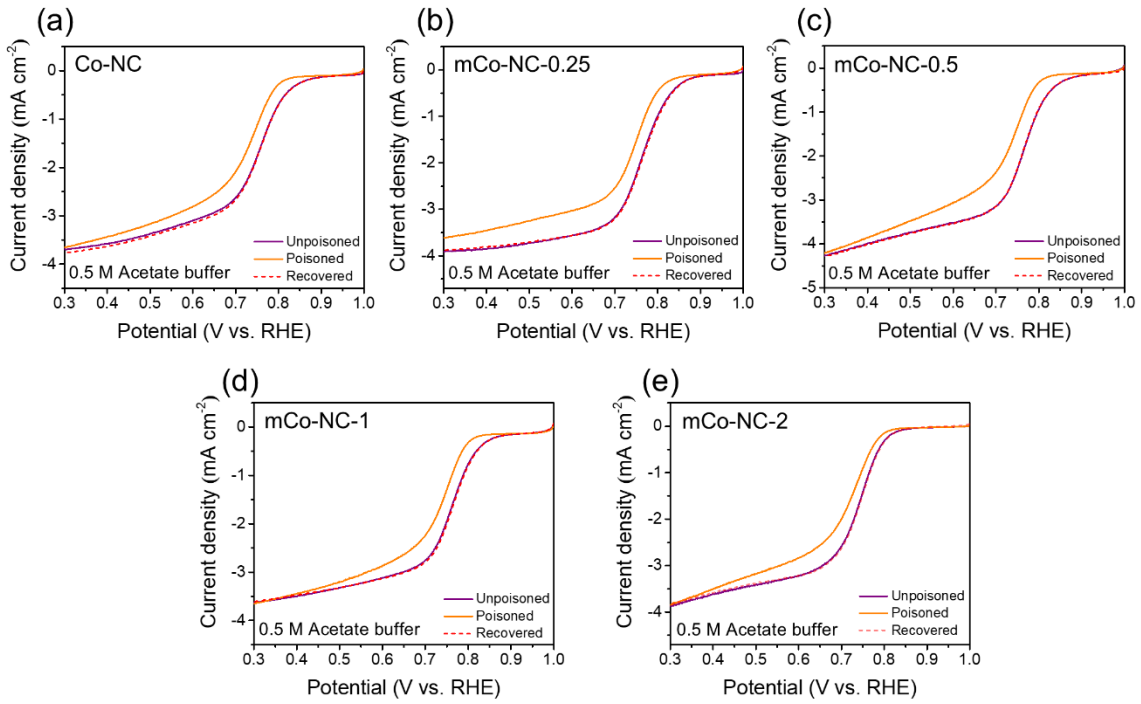

Figure S10. ORR polarization curves of nitrite adsorption/desorption in O_2-saturated 0.5 M acetate buffer at a rotation speed of 1600 rpm with a scan rate of 5 mV s^{-1} for: (a) Co-NC, (b) mCo-NC-0.25, (c) mCo-NC-0.5, (d) mCo-NC-1, and (e) mCo-NC-2.

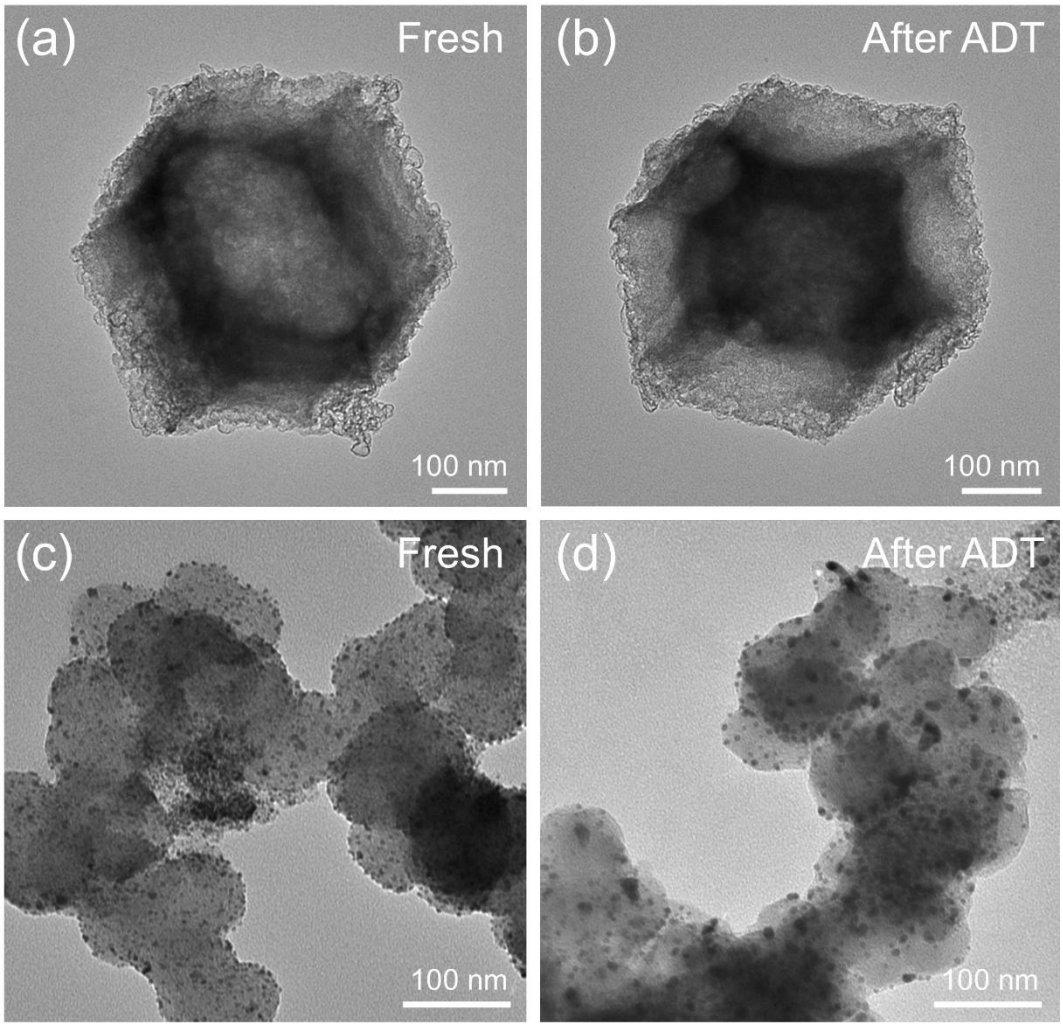

Figure S11. TEM images of (a, b) mCo-NC-1 and (c, d) Pt/C before and after ADT.

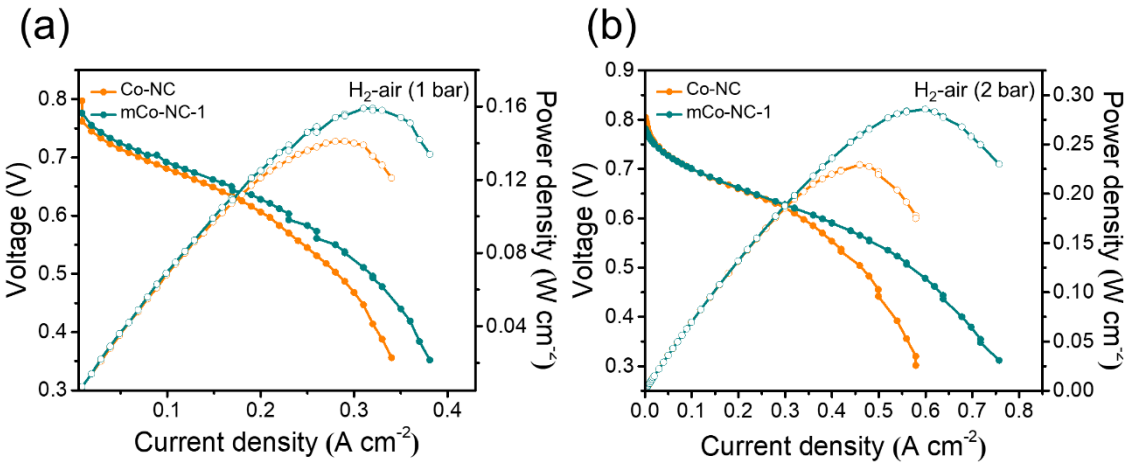

Figure S12. H_2/air PEMFC polarization curves of Co-NC and mCo-NC-1 cathodes at (a) 1 bar and (b) 2 bar. Test conditions: Cathode catalyst loading 0.5 mg cm^{-2} for Co-N-C, 5 cm^2 active area, Nafion 211 membrane, 100% relative humidity (RH).

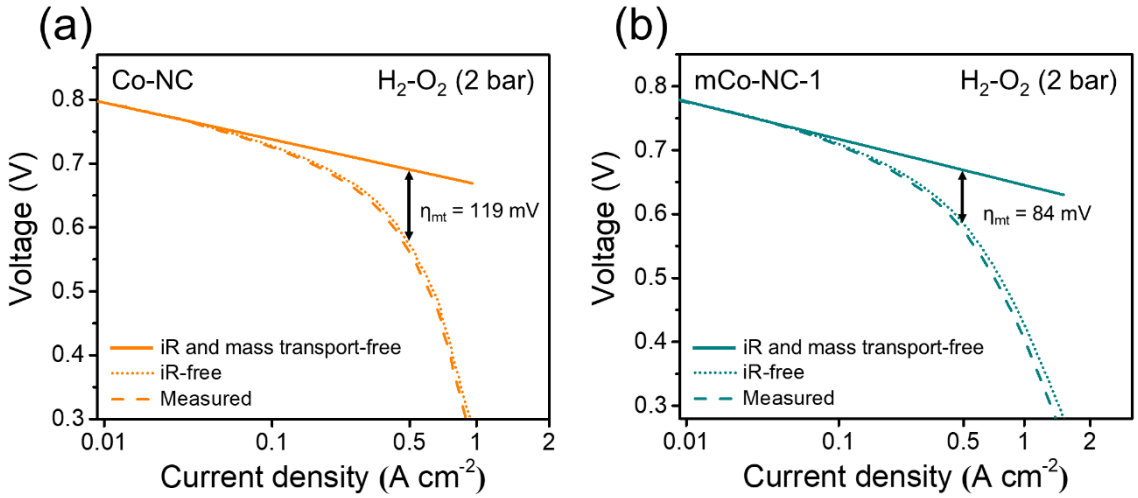

Figure S13. Mass transport overpotential of (a) Co-NC and (b) mCo-NC-1 under 2 bar H_2/O_2 conditions.

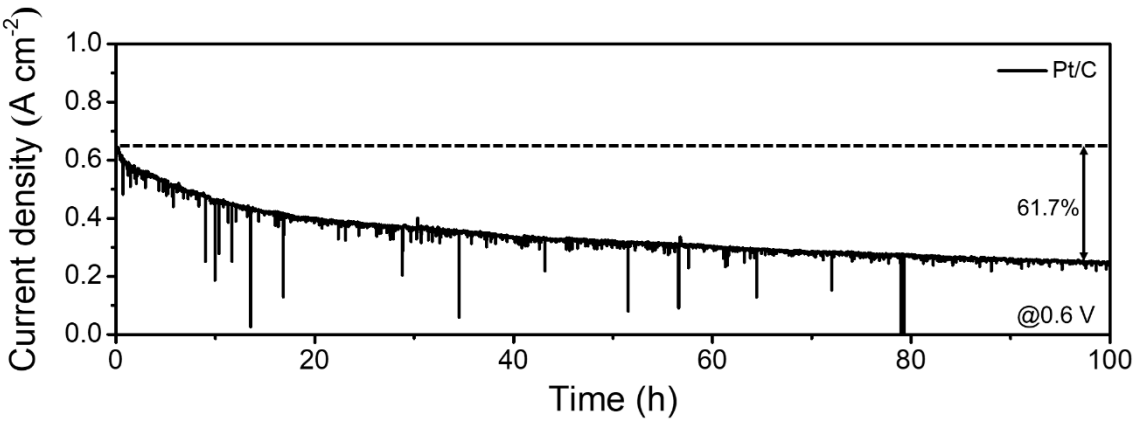

Figure S14. Fuel cell durability test at 0.6 V over 100 hours for Pt/C cathode MEA.

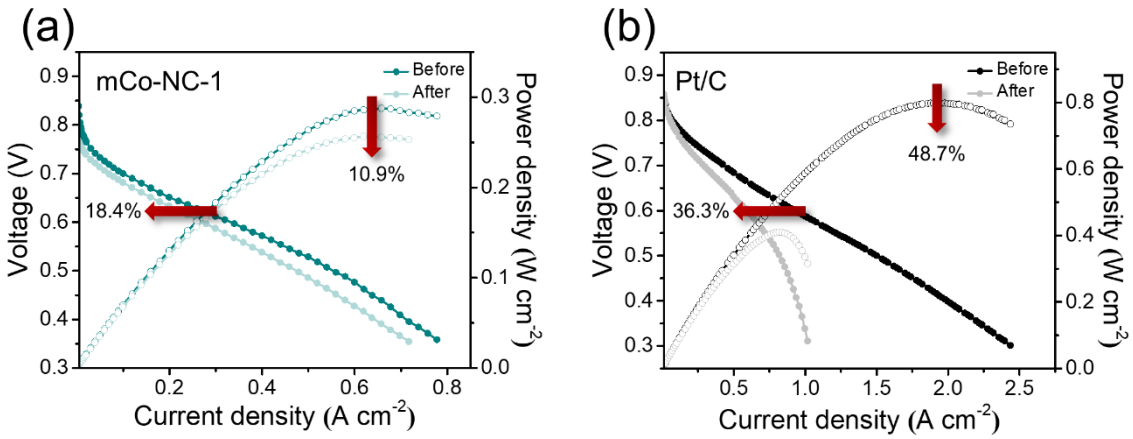

Figure S15. H_2/O_2 PEMFC polarization curves of (a) mCo-NC-1 and (b) Pt/C before and after durability tests. Test conditions: Cathode catalyst loading 0.5 mg cm^{-2} for Co-N-C and 0.2 mg_{Pt} cm^{-2} for Pt/C, 5 cm^2 active area, Nafion 211 membrane, 100% relative humidity (RH).

Table S1. Variation of pore structures in Co-NC catalysts with and without melamine.

Samples	S_{BET} (m^2 g^{-1})	Micropore area (m^2 g^{-1})	External area (m^2 g^{-1})	Proportion of external area*
Co-NC	1123	812	311	27.69%
mCo-NC-0.25	1001	681	320	31.97%
mCo-NC-0.5	1011	683	328	32.44%
mCo-NC-1	1067	574	493	46.20%
mCo-NC-2	548	0	548	100.00%

*Proportion of external area was determined based on BET surface area for each sample.

Table. S2 Comparison of onset potential, half-wave potential, limiting current density, and Tafel slope of all catalysts in 0.1 M $HClO_4$.

Samples	E_{onset} (V vs. RHE)	$E_{1/2}$ (V vs. RHE)	i_L (mA cm^{-2})	Tafel slope (mV dec^{-1})
Co-NC	0.782	0.706	4.73	99
mCo-NC-0.25	0.797	0.722	4.95	80
mCo-NC-0.5	0.801	0.738	5.19	88
mCo-NC-1	0.820	0.770	5.29	76
mCo-NC-2	0.757	0.696	4.99	62
Pt/C	0.841	0.775	5.28	70

Table S3. Electrolyte, charge transfer, diffusion resistance from EIS measurements.

Samples	R_s (Ω)	R_{ct} (Ω)	R_D (Ω)
Co-NC	19.20	155.38	-
mCo-NC-0.25	20.24	134.64	-
mCo-NC-0.5	19.39	136.96	-
mCo-NC-1	24.29	125.20	-
mCo-NC-2	19.11	162.76	286.84

Table S4. Catalyst site density, TOF, and cobalt utilization from nitrite stripping experiments.

Samples	Q_{strip} (C g^{-1})	SD (μmol g^{-1})	TOF@0.8 V (s^{-1})	Cobalt contents* (wt%)	Cobalt utilization**
Co-NC	21.27	44.09	0.48	2.00	12.99%
mCo-NC-0.25	29.10	60.31	0.50	2.29	15.52%
mCo-NC-0.5	34.54	71.61	0.45	2.32	18.19%
mCo-NC-1	37.11	76.93	0.31	2.49	18.21%
mCo-NC-2	9.47	19.63	0.36	6.89	1.68%

* Determined by ICP-AES.

** Calculated based on SD and Co contents.

Table S5. Area-specific and mass-specific performance of mCo-NC-1 and Pt/C in PEMFCs.

Samples	Areal specific performance		Mass specific performance*	
	P_{max} (W cm^{-2})	$i_{0.6\,V}$ (A cm^{-2})	P_{max} (W g^{-1})	$i_{0.6\,V}$ (A g^{-1})
Pt/C	0.80	0.93	4.00	4.65
mCo-NC-1	0.33	0.42	26.51	33.73

* Calculated by weight of Pt or Co metal, and Co content determined by ICP-AES.

Table S6. Comparative summary of PEMFC performance of Co-based non-precious metal catalysts reported in literature.

Catalyst	Loading (mg cm^{-2})	Conditions		P_{max} (mW cm^{-2})	Ref.
		Fuel	Pressure		
mCo-NC-1	0.5	H_2-O_2	1 bar	327	**This work**
			2 bar	442	
		H_2-air	1 bar	159	
			2 bar	286	
Co/Zn(mlm)$_2$-P	1.6	H_2-O_2	2 bar (O_2)	374	[S1]
Co-corrole/C-700	3.0	H_2-O_2	2 bar	275	[S2]
Co@SACo-N-C-10	4.0	H_2-O_2	1 bar	420	[S3]
		H_2-air	1 bar	230	
Co(mIm)-NC(1.0)	5.8	H_2-O_2	1 bar	640	[S4]
		H_2-air	1 bar	320	
1.6%CoNC-ArNH$_3$	3.0	H_2-O_2	1.5 bar	440	[S5]
			3.0 bar	750	
		H_2-air	1.5 bar	221	
			3.0 bar	305	
CoTMPP	4.0	H_2-O_2	20 N cm^{-2}	150	[S6]
20Co-NC-1100	4.0	H_2-O_2	30 psi	560	[S7]
		H_2-air	30 psi	280	
CoTPP	4.0	H_2-O_2	30 psi	150	[S8]
Co-N-PCN	4.0	H_2-O_2	1 bar	710	[S9]
		H_2-air	1 bar	400	
Co-N-C@F127	4.0	H_2-O_2	1 bar	870	[S10]
Co-N/C-1/4.4	3.5	H_2-O_2	1 bar	1000	[S11]
		H_2-air	1 bar	490	

2. References

[S1] W. Wu, Q. Zhang, X. Wang, C. Han, X. Shao, Y. Wang, J. Liu, Z. Li, X. Lu, M. Wu, ACS Catal., 2017, 7, 7267-7273.

[S2] C. Zhang, H. Yang, D. Zhong, Y. Xu, Y. Wang, Q. Yuan, Z. Liang, B. Wang, W. Zhang, H. Zheng, T. Cheng, R. Cao, J. Mater. Chem. A, 2020, 8, 9536-9544.

[S3] Y. Meng, Y. Huang, G. Huang, Y. Song, RSC Adv., 2023, 13, 28148-28157.

[S4] O. Pop-Georgievski, D. Kubies, J. Zemek, N, Neykova, R. Demianchuk, E. M. Chánová, M. Šlouf, M. Houska, F. Rypáček, Beilstein J., 2015, 6, 617-631.

[S5] C. Young, R. R. Salunkhe, J. Tang, C.-C. Hu, M. Shahabuddin, E. Yanmaz, M. S. A. Hossain, J. H. Kim, Y. Yamauchi, Phys. Chem. Chem. Phys., 2016, 18, 29308-29315.

[S6] T. Feng, W. Liao, Z. Li, L. Sun, D. Shi, C. Guo, Y. Huang, Y. Wang, J. Cheng, Y. Li, Q. Diao, Nanoscale Res. Lett., 2017, 12, 595.

[S7] X. Zhang, S. Zhang, Y. Yang, L. Wang, Z. Mu, H. Zhu, X. Zhu, H. Xing, H. Xia, B. Huang, J. Li, S. Guo, E. Wang, Adv. Mater., 2020, 32, 1906905.

[S8] K. Qiu, G. Chai, C. Jiang, M. Ling, J. Tang, Z. Guo, ACS Catal., 2016, 6, 3558-3568.

[S9] K. Huang, P. Xu, X. He, R. Wang, Y. Wang, H. Yang, R. Zhang, M. Lei, H. Tang, ChemElectroChem, 2020, 7, 3341-3346.

[S10] R. Li, Z. Wei, X. Gou, ACS Catal., 2015, 5, 4133-4142.

[S11] L. Chen, X. Liu, L. Zheng, Y. Li, X. Guo, X. Wan, Q. Liu, J. Shang, J. Shui, Appl. Catal. B, 2019, 256, 117849.

*****